

Optical, mechanical and electro-optical design of an interferometric test station for massive parallel inspection of MEMS and MOEMS

Kay Gastinger ^{(1)*}, Karl Henrik Haugholt ⁽¹⁾, Malgorzata Kujawinska ⁽²⁾, Michal Jozwik ⁽²⁾,
Christoph Schaeffel ⁽³⁾, Stephan Beer ⁽⁴⁾

⁽¹⁾ SINTEF IKT Optical measurement systems and data analysis, N-7465 Trondheim, Norway,

⁽²⁾ Institute of Micromechanics and Photonics, Warsaw University of Technology, 8 Sw. A. Boboli St.,
PI-02-525 Warsaw, Poland

⁽³⁾ IMMS, Ehrenbergstr. 27, D-98693 Ilmenau, Germany

⁽⁴⁾ CSEM Centre Suisse d'Electronique et de Microtechnique SA, Technoparkstr. 1, CH-8005 Zurich, Switzerland

ABSTRACT

The paper presents the optical, mechanical, and electro-optical design of an interferometric inspection system for massive parallel inspection of MicroElectroMechanicalSystems (MEMS) and MicroOptoElectroMechanicalSystems (MOEMS). The basic idea is to adapt a micro-optical probing wafer to the M(O)EMS wafer under test. The probing wafer is exchangeable and contains a micro-optical interferometer array. A low coherent and a laser interferometer array are developed. Two preliminary interferometer designs are presented; a low coherent interferometer array based on a Mirau configuration and a laser interferometer array based on a Twyman-Green configuration. The optical design focuses on the illumination and imaging concept for the interferometer array. The mechanical design concentrates on the scanning system and the integration in a standard test station for micro-fabrication. Models of single channel low coherence and laser interferometers and preliminary measurement results are presented. The smart-pixel approach for massive parallel electro-optical detection and data reduction is discussed.

Keywords: Low Coherence Interferometry, Laser Interferometry, Smart Pixel Camera, Micro-Optics, MEMS testing

1. INTRODUCTION

Micro-fabrication of Micro(Opto)ElectroMechanicalSystems (M(O)EMS) on silicon or glass wafers are today constitutes large volumes. Each wafer contains from tens up to several thousand devices. In the production process there is a need to test both passive parameters (i.e. x-y-(z) dimensions) and active parameters (e.g. resonance frequencies, deformations) of the structures.

Test systems for wafer-based M(O)EMS testing are available on market today. However, in particular the measurement of active parameters is time consuming, and thus not well suited for in line testing in mass production. This is caused by the serial inspection approach. Each M(O)EMS-structure is tested individually where translation stages are used to move the inspection system from structure to structure.

Furthermore today's inspection systems are inflexible and expensive. Each inspection task requires a separate test station leading to high investment costs and occupies expensive clean room space. New multifunctional inspection concepts are required based on the same technological platform as the rest of the production chain.

Non-contact methods are needed when measuring non-electrical parameters of M(O)EMS because of the fragility of the microscopic structures [1]. Optical methods are non-intrusive and non-tactile and thus well suited for this purpose. Optical microscopy combined with interferometry is a versatile tool for the testing of M(O)EMS in micro-fabrication. Interferometry can be applied for the passive characterisation of the shape, as well as for the active characterisation of deformation [2] and resonance frequencies [3] of M(O)EMS structures.

Testing for quality control is thus the bottle neck in M(O)EMS production, in particular where 100% quality control is required. The major challenge is how to bridge the gap between mass production of M(O)EMS and single channel

* phone +47 73590457, email: kay.gastinger@sintef.no

approach of today's standard equipment, and also the requirement of multifunctionality on the same technological platform as in the rest of the production chain. A way to significantly increase the throughput rate and cost efficiency is a parallel approach to the testing process. The aim is to test several or all M(O)EMS structures within a single measurement cycle. Camera based techniques need to be applied to enable full-field measurements. Multifunctionality can be implemented e.g. by the use of exchangeable sensor heads.

2. INSPECTION CONCEPT

The EU-project SMARTIEHS develops a novel inspection approach solving all challenges given above [4]. By introducing a wafer-to-wafer inspection concept the parallel testing of several dozens of M(O)EMS structures within one measurement cycle becomes possible. To obtain this an exchangeable micro-optical probing wafer is adapted and aligned with the M(O)EMS wafer under test. The probing wafer comprises an interferometer array. The configuration, spacing and resolution of the interferometer array are designed for each specific application. Furthermore also the illumination, imaging and excitation modules are modular and can be moved from one interferometer array to the other. The modules can thus be interchanged if the spatial distribution of the MOEMS structures or changed functionality requires this. The array configuration can be non-regular and optimised for time-efficient inspection strategies. More than 100 interferometers can thus be arranged on an 8-inch wafer and decrease the inspection time of a wafer by a corresponding factor.

The wafer-to-wafer concept addresses the production of complete interferometers in an array arrangement by standard micro-fabrication technologies. All the interferometers in one array have to be precisely spaced within micrometer tolerances. Additionally, as each interferometer consists of multiple functional optical layers, the layers need to be arranged at a certain distance with micrometer accuracy. Possible approaches to solve this challenge are stacking of different micro-optical wafers to a "semi-monolithic" block or applying double sided fabrication of elements on one wafer.

In this paper the multifunctionality of the system is demonstrated by two different probing wafer configurations, a 5x5 array of low coherent interferometers (LCI) and a 5x5 array of laser interferometers (LI). An array of 5x5 smart-pixel cameras is designed for the detection of the interferometer signals. The cameras feature optical lock-in detection at the pixel level [5].

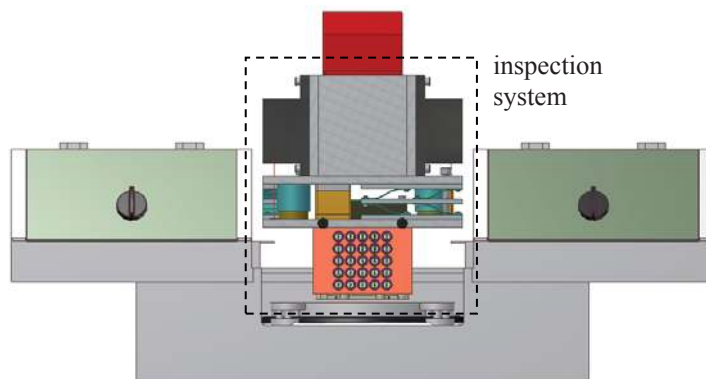


Figure 1 CAD 3D representation of the SUSS test station (PA200) for M(O)EMS testing, with the inspection system attached at the scope mount of the prober.

The inspection system is mounted on a commercially available wafer handling and positioning system (SUSS prober – PA 200 with probe shield). The M(O)EMS wafer is mounted and positioned using the wafer chuck of the prober. Figure 1 shows a sketch of the prober and the inspection system integrated on the prober.

The instrument configuration is shown in Figure 2. It comprises the two different interferometer arrays. The left side of the image shows the low coherent interferometer and the right side the laser interferometer array. The light sources are arranged in an array and positioned on each side of each interferometer unit. The light is guided by a beam splitter towards the probing wafer.

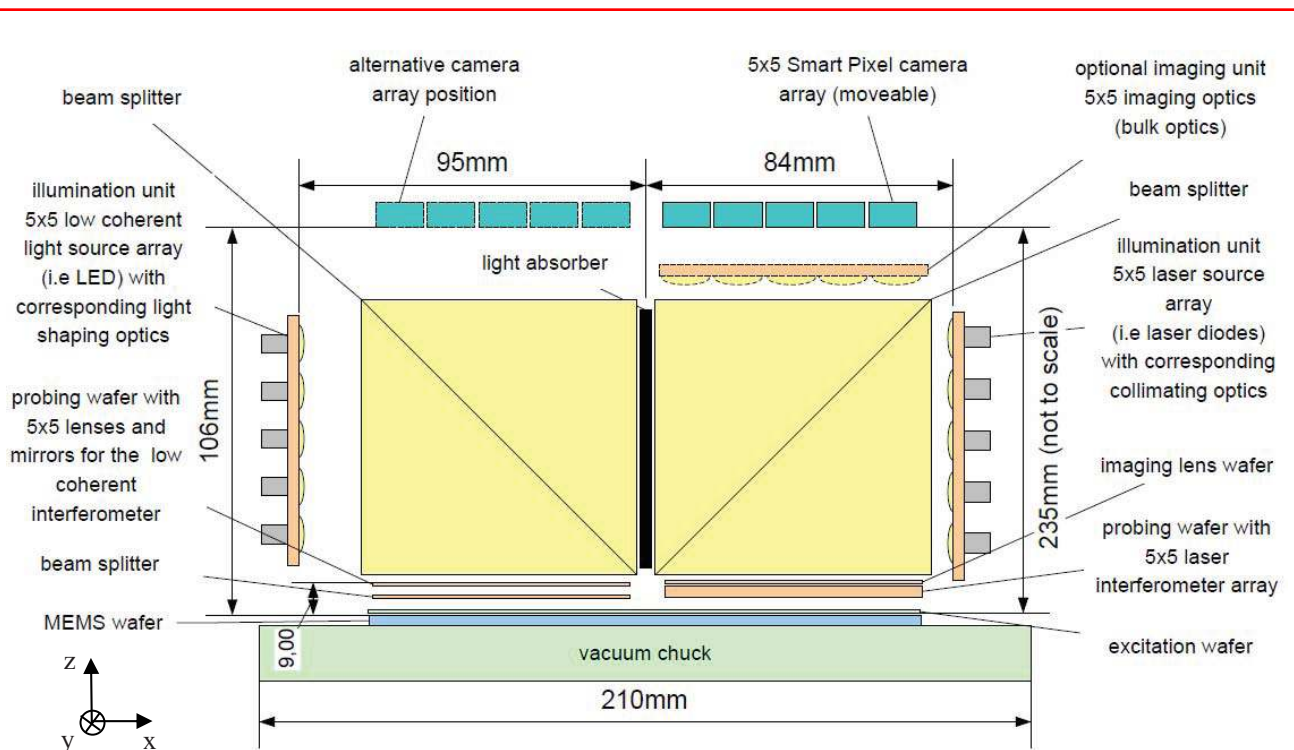


Figure 2 SMARTIEHS instrument configuration: Side view with dimensions. The vacuum chuck is part of the SUSS prober used for mounting the M(O)EMS wafer.

The interference signals are generated in the micro-optical interferometers which are fabricated in a regular matrix on a 4-inch wafer stack. Two different interferometer approaches are pursued; a refractive Mirau type and a diffractive Twyman-Green type interferometer. The refractive design will be used for low coherence interferometry to measure the shape and deformation of the M(O)EMS structures. The diffractive design will be applied for vibration analysis using laser interferometry to find the resonance frequency and spatial mode distribution. Furthermore the LI will be applied to measure shape and deformations on smooth surfaces.

A glass wafer containing mini-lenses produced by standard micro-fabrication processes is used for the imaging of the interference fringes towards the camera. A distributed array of 5x5 smart pixel imagers detects the interferometric signals. The signal processing is based on the “on pixel” processing capacity of the smart pixel camera array, which can be utilised for phase shifting or envelope maximum determination. Each micro-interferometer image will thus be detected by a 140 x 140 pixels sub-arrays distributed in the imaging plane.

An excitation system for the M(O)EMS structures is needed for active testing. A glass wafer consisting of Indium Tin Oxide (ITO) electrodes is applied for electrostatic excitation of the resonance frequency of the structures [5]. For the measurement of deformation the active area on the M(O)EMS is excited either electrostatic by the ITO wafer or using a tailor made pressure chuck.

3. SYSTEM DESIGN

3.1. Mechanical design

The semiautomatic prober system SUSS PA200 supplies a chuck movement in x, y, z and rz (r - rotation). This is used for the positioning and horizontal scanning of the M(O)EMS wafer. Furthermore the scope adapter of the prober can be moved in x, y and z. This adapter is used to mount the inspection system.

Figure 3 shows a CAD 3D representation of the inspection system. The system can be divided into two main components – a drive unit and an optical unit. The drive unit carries the high precision drive and the springs.

The raw positioning of the inspection system in z is done by the scope drive. However the linearity and positioning accuracy of the scope drive is not sufficient for the interferometric measurements.

Therefore a separate high precision drive unit is designed. This ensures the parallel alignment of the probing wafer with the M(O)EMS wafer by adjusting r_x and r_y . Furthermore the high precision drive has to perform a highly uniform movement and positioning in z. LCI requires a scan over a range of 1mm with a linearity of 1%. LI requires positioning accuracies with a measurement error $<10\text{nm}$ and a high frequency position stability in the nanometer range.

Those high requirements are realised in the design concept by integrating three single drive subsystems. A voice coils based driving system is selected to obtain a travel range of 1mm. Three commercial interferometer systems deliver position signals with an accuracy of 3nm which enables a positioning accuracy of 10nm. The controller of the drive system will be realized by a rapid controller prototyping system, e.g. *dSpace*.

The two interferometer modules are mounted on the optical unit. The design enables various adjustment possibilities of the different optical components.

The mechanical guiding in z direction is realized by three parallel leaf spring systems. The doubled configuration of leaf springs compensates a possible movement in x- and y-directions. Hence, the leaf spring system assures a guided movement only in z as required. The leaf springs are pre-stressed to compensate the weight of the optical unit.

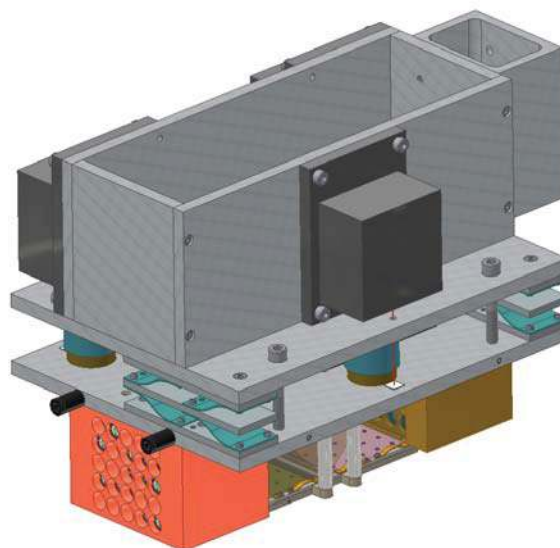


Figure 3 CAD 3D representation of the inspection system, above: drive unit, below: optical unit

3.2. Optical design

The optical unit of the inspection system consists of two optical modules, one containing the LI array and one the LCI array. Figure 4 shows a CAD 3D representation of the optical unit.

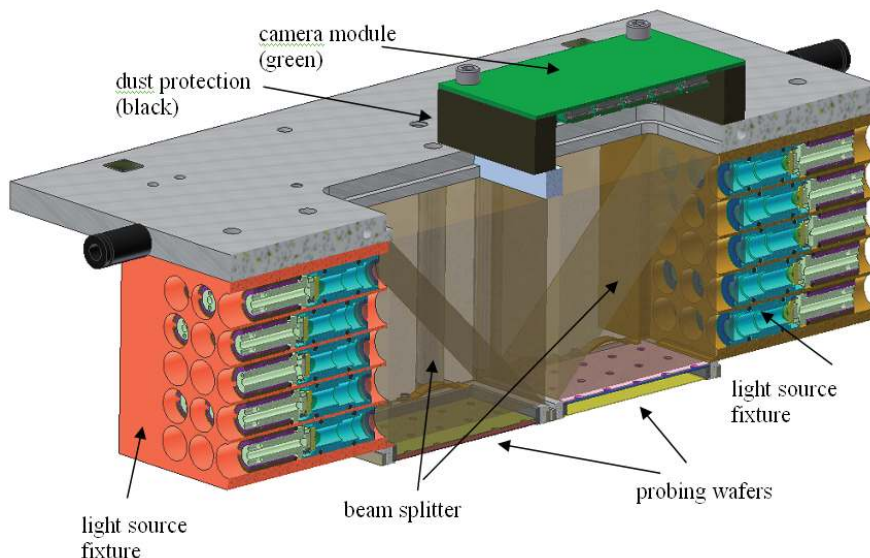


Figure 4 Optical unit of the inspection system consisting of the low coherence interferometer module (left) and the laser interferometer module right. The smart pixel camera (on top) is moveable between the two modules. It is shown in the position for detection of the laser interferometer signals.

The light source illuminates the M(O)EMS object via a cube beam splitter. The centre of the illumination aperture is thus aligned with the centre of the imaging lens and the centre of the object along the optical axis. The optical axis is deflected 90° by the beam splitter. The centre of the active area in the corresponding camera images the M(O)EMS structure under inspection.

Care has been taken to mount the probing wafers without introducing tension in the wafers. Any bending of the wafers will introduce variations in the optical path length in the interferometers and misalign the optical system.

3.2.1. Illumination

The light sources have an adjustable beam angle. The light source can be eccentrically rotated and moved along the optical axis. Thus the illumination can be conditioned. The illumination modules are configured as a matrix of light sources, i.e. light emitting diodes (LED) or laser diodes (LD). Alternatively, a single source can be distributed over the entire test wafer area. The designs described in this paper are based on the matrix approach. Figure 5 shows the position of the light source array in a 3D representation

3.2.2. Smart pixel camera

The smart pixel camera modules can be individually focused. This enables the compensation of deviations of the nominal focal lengths that may occur in the production of the mini-lenses. Figure 5 shows an example of the mechanical arrangement of the camera for this case. By allowing for a production tolerance of $\pm 4\%$ in focal lengths, each smart camera imager needs an adjustment of $\pm 20\text{mm}$. The imaging optics has a magnification of 9x. The imaging system is designed without an intermediate image. The field of view is $600 \times 600 \mu\text{m}^2$.

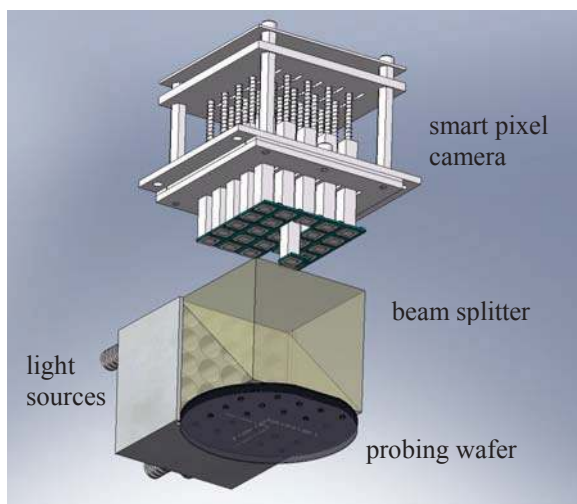


Figure 5 CAD 3D representation of one of the optical units connected with the camera array.

3.2.3. Pitch of interferometer wafer array

The pitch of the interferometer arrays is adapted to the pitch of the structures on the M(O)EMS wafer under test. The interferometer pitch is much larger than the pitch of the M(O)EMS structures, because of the size of the imagers. The structures are therefore tested in an interlaced manner. In the case presented here we use an interferometer pitch of 13,76mm. The probing wafer inspects thus each eighth structure in the array. The structures in between are then measured by positioning the interferometer array above the corresponding neighbor structure and thus scanning consecutively all objects on the wafer.

For other M(O)EMS wafers with a different pitch new probing wafers will have to be manufactured. However, smaller pitch variations can be compensated by adopting the magnification and focusing of the imaging system.

3.3. Low coherence interferometer

For low coherence interferometry a micro-optical approach of a Mirau configuration is applied. The illumination is realized by an array of Light-Emitting Diodes (LED). Each illumination system consists of an LED, a lens and an aperture. The LED is slightly defocused imaged onto the imaging lens. Camera and illumination aperture are, seen from the object side, “virtually” positioned in the same vertical and horizontal position.

Figure 6 shows the preliminary design of the interferometer array. It consists of 2 separate wafers. The lens wafer is carrying the imaging lenses and the reference mirror. The beam splitter wafer is a glass wafer with a partly reflective coating on the upper side.

The imaging lens consists of a refractive micro-fabricated mini lens with a diameter of 2,5mm. The beam splitter wafer divides the incoming light into a reference beam and an object beam. The reference beam is reflected by the reference

mirror positioned in the centre part of the lens. The object beam is reflected back from the M(O)EMS structure under test. Both beams are interfering in the beam splitter wafer. The interference fringes are imaged onto the camera, where the smart pixels detect and demodulate the interference signal.

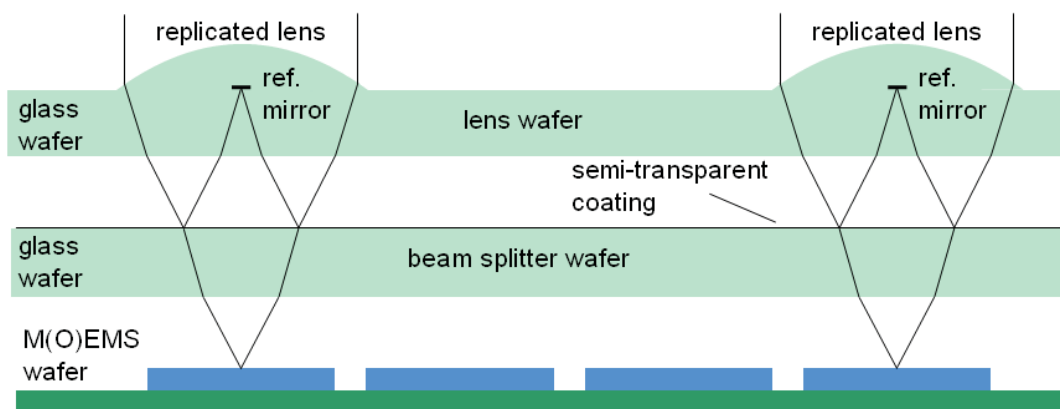


Figure 6 Preliminary design of the low coherent Mirau interferometer configuration in a matrix approach.

3.4. Laser interferometer

LI has a Twyman-Green interferometer configuration as it is proven to be an efficient setup for active full-field M(O)EMS testing [7][8]. A Twyman-Green interferometer is a two-beam interferometer, illuminated by a beam with a plane waveform generated by a point source and a collimator. The preliminary design of the LI is shown in Figure 7.

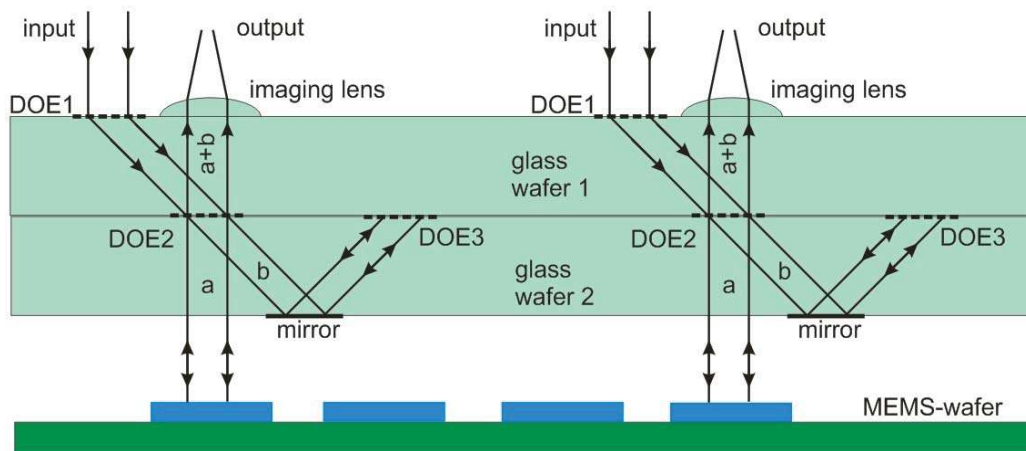


Figure 7 Preliminary design of the laser based Twyman-Green interferometer configuration in a matrix approach.

The illumination system is realized by a laser diode matrix and an aspheric lens. One laser diode is dedicated to one interferometer channel.

The interferometer is formed from two wafers. The top wafer is a thick glass wafer with a diffractive optical element DOE1 etched on the surface. This grating diffracts the incident collimated beam in order to illuminate the beam splitting diffraction structure DOE2. The second wafer is also a glass wafer and contains DOE2, DOE3 and a mirror surface. DOE 2 divides the incoming light in object and reference beam. The transmitted light of DOE2 forms the reference beam. The DOE3 plays a role of a reference mirror. The diffracted light of DOE2 is directed towards the object surface and forms the object beam. Both beams are recombined by DOE2 and interfere. The interference pattern is imaged by the imaging lens integrated on the glass wafer surface and captured by the camera. The full image of the smart pixel camera consists of the matrix of sub-images given by the interferometer matrix.

3.5. Smart Pixel Camera design

Figure 8 shows the configuration of the imager array camera. The smart pixel imagers are placed in a 5x5 matrix at the camera module which transfers the images via a high speed frame grabber to the PC. The pitch between the imager chips is adapted to the interferometer pitch.

Each of the 5×5 interferometric channels is equipped with a smart-pixel CMOS imager for detection of the optical signal. Every imager features 140×140 pixels (150×150 including black and reference pixels), which increases the parallelism to a total resolution of about half a million interferometric sub-channels.

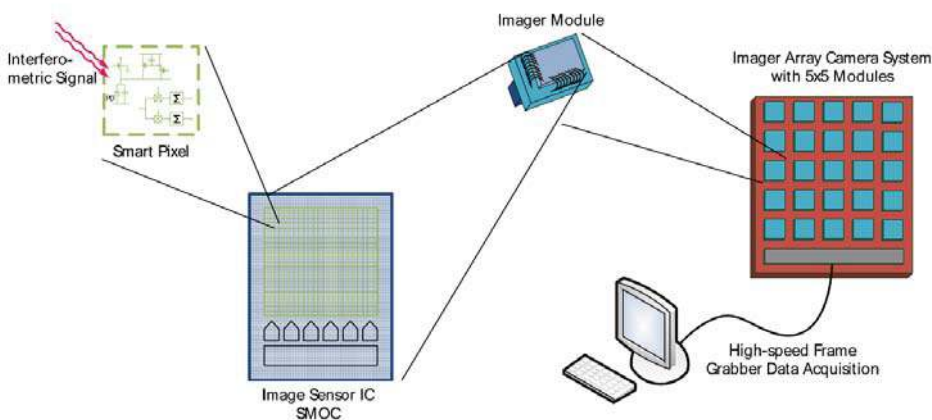


Figure 8 Configuration of the smart-pixel camera.

The object measurement time of LCI with scanning of the optical path length is usually limited by the frame rate of the detector imager. The interferogram is an amplitude modulated signal containing the depth information of the sample in its envelope. For every scan distance corresponding to the period of the optical system, i.e. half of the illumination peak wave length, several frames are acquired limiting the scan speed to some micrometers per second.

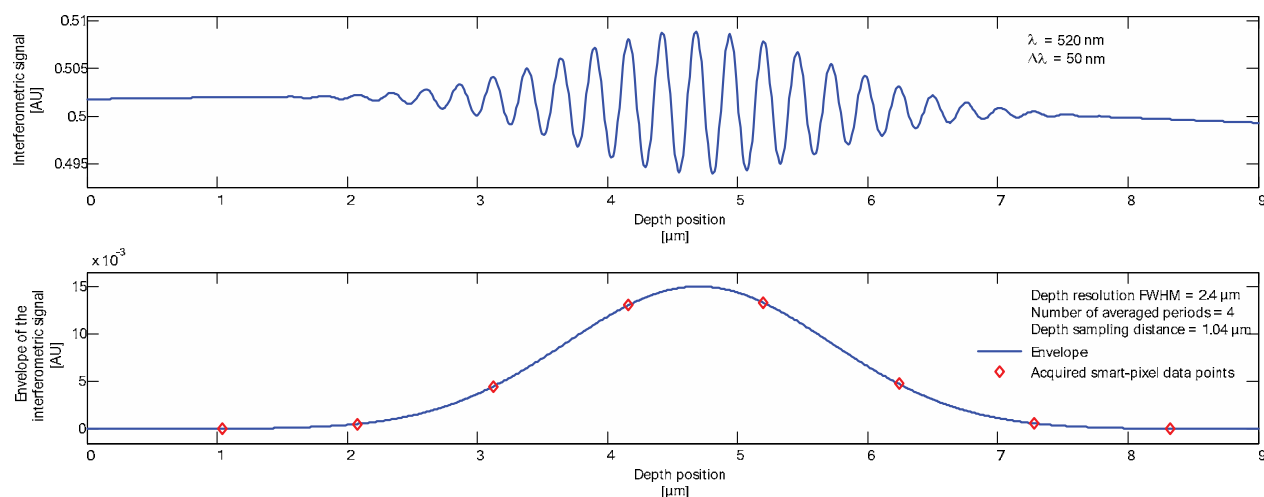


Figure 9 Simulated LCI signal, envelope, and smart-pixel acquired measurement points of one sub-channel detecting a surface at a depth of $4.7 \mu\text{m}$ (only depth range shown where interference fringes appear).

The developed smart-pixel architecture allows the demodulation of the electro-optical signal at the detection level with demodulation frequencies up to 100 kHz. The demodulated signal is averaged over a few periods and then read out to

the control system (Figure 9). The data volume is drastically reduced and the depth scan speed is increased without the need of a high imager read-out frame rate.

Figure 10 shows the I-Q direct demodulation principle implemented within every pixel. The optical signal striking a pixel is detected and converted into an electrical signal on the photo diode. A background suppression circuit avoids saturation of the pixel at high illumination levels and small input signal contrast. The signal is integrated and sampled. These signal samples are multiplied by a signal of the same frequency and averaged on two paths, phase shifted by $\pi/2$ with respect to each other. A sample and hold stage in both circuit branches allows simultaneous demodulation and read-out, which means that while the stored values are read out of the imager pixel field, the input signal is demodulated to already generate the next values. The outputs of the two paths are read out of the imager to the PC and the envelope amplitude is calculated. A three-dimensional model of the imaged object is then generated from this data.

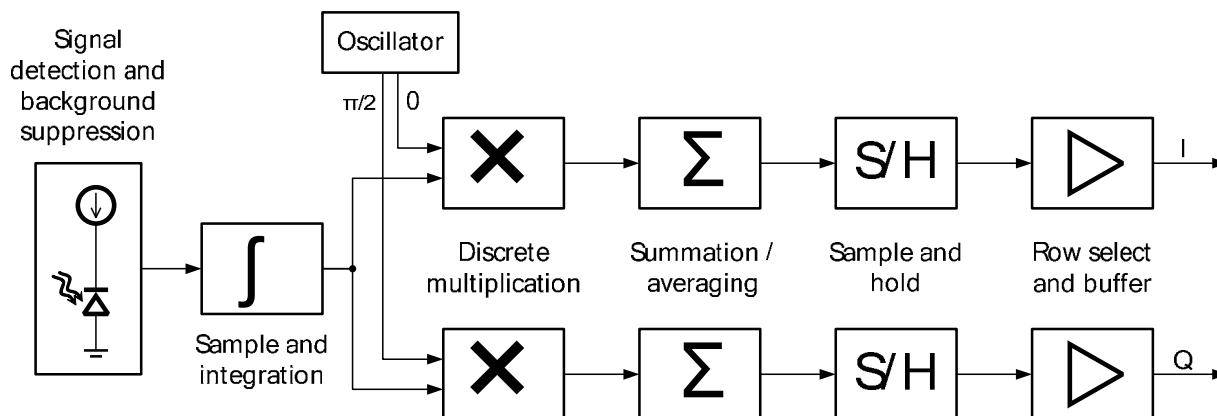


Figure 10 I-Q direct demodulation principle of the smart-pixel.

The versatile electronic circuit at the pixel level not only allows amplitude demodulation but also the extraction of the modulation phase. Furthermore, conventional grey-level images can be acquired. The architecture is therefore well suited not only for LCI but also for phase-stepping LI and vibrometry.

4. SINGLE CHANNEL DEMONSTRATORS

4.1. Low coherent interferometer

4.1.1. Experimental setup

A single channel LCI was realized to identify critical parameters, tolerances and to characterize the performance of the system. The set up has been step wise improved to get as close as possible to the designed solution and is based on a wafer approach.

Figure 11 shows the configuration of the experimental setup. In the left image a sketch of the single channel Mirau configuration is shown. The illumination is based on a high power LED with a rather large active area ($1,5 \times 1,5 \text{mm}^2$). The power of the LED is 50mW. The spectrum of the LED has a centre wavelength of 532nm and a FWHM of 35nm. The illumination unit is realised by a doublet with a focal length of 25mm and an aperture of 10mm.

The light from the imaging aperture is guided via a non-polarizing beam splitter towards the interferometer. This realises a concentric illumination. To keep the system as simple as possible polarizing and birefringent components are avoided. The upper wafer is a 4'' glass wafer with gold mirrors and imaging apertures of different sizes. The lower wafer acts as beam splitter and is realised by a semi transparent metal layer on the upper side of a glass wafer. The wafers are stacked using an aluminium holder and three glass spacers. The thickness of the spacers was modelled by ZEMAX and the spacers are cut from a suitable sheet glass. A commercially available, precision moulded, spherical

singlet lens was placed on top of the mirror wafer as imaging lens, because the micro-fabricated mini lenses will be produced later in the project.

The interference signal is detected by a standard CMOS colour camera (Micron).

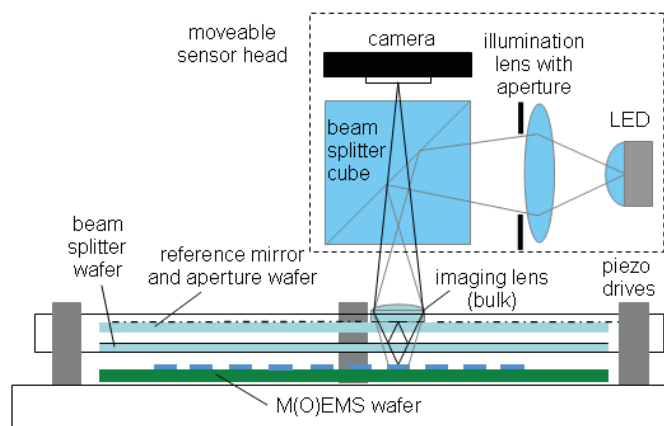


Figure 11 Experimental setup LCI, left: sketch of the wafer based Mirau configuration, right: photo of the setup.

4.1.2. Measurement results

Figure 12 shows the fringe pattern recorded with the configuration introduced above. The available lens fabrication technology restricts the lens diameter to ca 2,5mm. Therefore the selected imaging aperture on the upper wafer was 2,5mm. The field of view has a diagonal of ca 900 μ m. A circular reference mirror with a diameter of 900 μ m will be a substantial part of the aperture. However, a good fringe contrast is obtained.

The high frame rate of the smart pixel sensor demands high light intensity to take full advantage of its capabilities. Therefore the light budget is critical. The sensor requires an optical power of 2mW on the active area of the imager to work with a typical demodulation frequency. This is not realistic with the given configuration and LEDs as light sources. In the setup 50 μ W have been measured. This would allow a demodulation frequency of about 1kHz, which is on the lower end of the frequency range. Superluminescence diodes (SLD) can be used as an alternative light source, leading to significant higher costs.

The intensity distribution across the field of view is nearly homogeneous. However, the intensity is slightly lower at the edge of the image.

Furthermore the influence of dispersion is investigated. A difference in the path length in glass of 100 μ m will completely extinguish the interference fringes.

The reflection of the “back” side of the reference mirror is the dominant source of stray light on the sensor. This will be considered in the optical design of the final interferometer configuration.

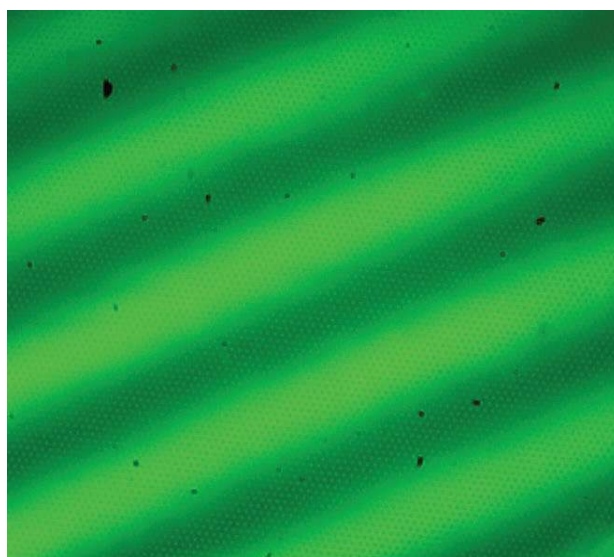


Figure 12 Fringe pattern obtained from a perforated membrane and recorded by the LCI single channel configuration.

4.2. Laser interferometer

4.2.1. Experimental setup

The single channel model of the LI interferometer has been built using separated, simple components located in free space (Figure 13 and 14). The illumination is realized by a laser diode LD with the wavelength of 635nm. The laser beam is collimated by lens C and reflected by the beam splitter cube BS in the direction of the optical setup. The configuration of the experimental setup has a similar functionality as the system proposed on Figure 7.

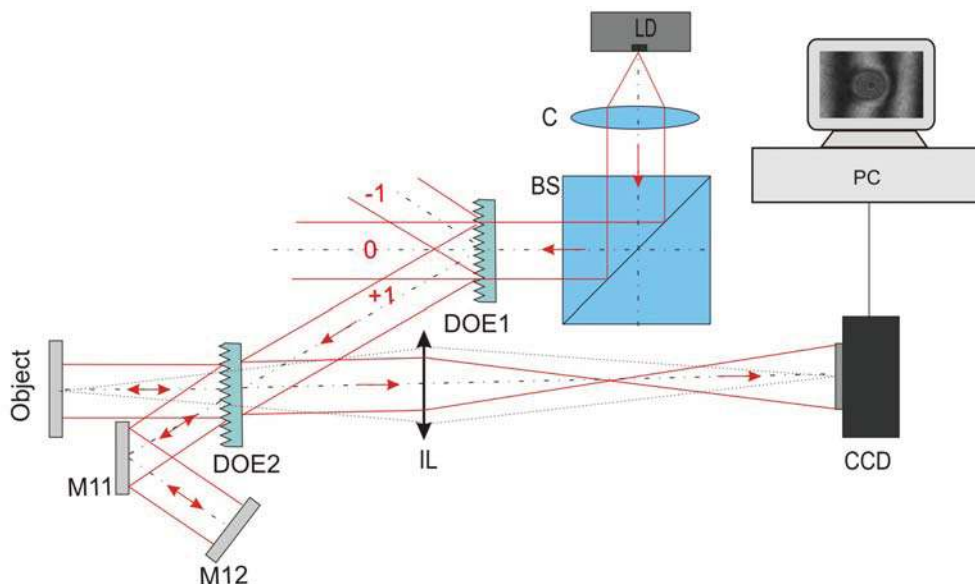


Figure 13 The scheme of LI interferometer with a single imaging lens.

It includes 2 diffraction gratings (in-coupling DOE1 and beam-splitting DOE2) only and a plane mirror M12 as the reference surface. Mirror M11 is an additional reflected surface. The recombined beams from object and reference mirror M12 are imaged on the CCD (Flea2 from Point Gray Research Inc.) by a single lens IL which magnifies the object and conjugate the object and camera CCD planes. The diffraction gratings are the high quality sinusoidal structures with a period of $1\mu\text{m}$. These parameters are significantly different to those required for the final solution. However they allow to provide the proof-of-principle of LI and to verify the main parameters and functionality of the proposed design. The optimized diffractive elements will be fabricated later in the project.

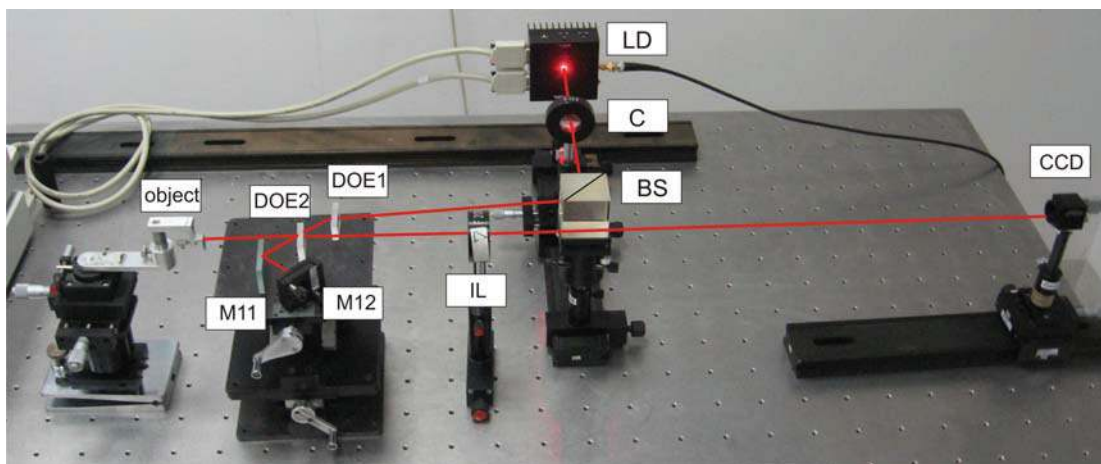


Figure 14 Photo of the LI experimental setup with indication of the elements and the optical path.

4.2.2. Measurement results

Using laser interferometry with one wavelength it is only possible to measure objects with continuous shape function. Surface steps higher than $\lambda/2$ cannot be measured properly, due to the mod- 2π phase ambiguity. Figure 15 shows fringe pattern recorded by the CCD camera. The laser interferometry configuration was tested by measuring the deflection of micro-membranes (diameter $800\mu\text{m}$) on a silicon wafer. The membranes are observed from the back side. The presented images show interferograms obtained from two membranes located in different regions at the MEMS wafer. The left membrane (Figure 15a) has a flat surface while the right membrane (Figure 15b) has a deformed surface with a deflection of app. 200nm. The contrast of the fringes is satisfactory and allows the further processing of the interference pattern. In the final system the analysis will be performed using its demodulation mode of the smart camera.

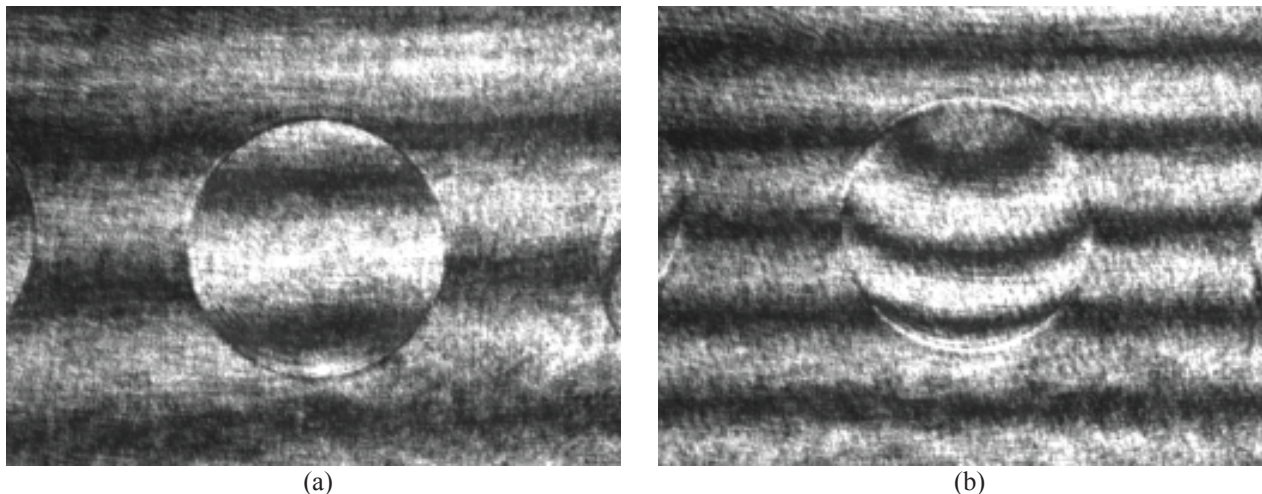


Figure 15 Interference fringes obtained on a (a) flat and (b) deflected membrane.

CONCLUSIONS

The presented inspection system realises a parallel approach for the production test of M(O)EMS. The instrument concept is based on a probing wafer inspecting more than 100 M(O)EMS structures within only one measurement cycle. The instrument concept enables thus the reduction of the measurement time by a factor of more than 100. Furthermore a multifunctional approach is demonstrated based on interchangeable probing wafers produced by standard micro-fabrication processes.

This multifunctional approach of the measurement concept allows the inspection of passive and active parameters within the same inspection system. Two different micro-optical interferometer configurations are presented; a Mirau type low coherent interferometer for shape and deformation measurements and a Twyman-Green type laser interferometer for the measurement of resonance frequency and the spatial vibration mode distribution.

Two single channel models are developed for the proof-of-principle of the micro-optical interferometer configurations. The results are promising even if the light budget in the low coherent interferometer is on the lower limit.

A novel distributed smart pixel camera is developed. It consists of a 5×5 matrix of smart pixel imager. Each imager has a 140×140 pixel resolution giving a total number of almost half a million interferometer channels. The smart pixel approach enables “on pixel” demodulation of the interference signal and contributes thus to data reduction and a short measuring time.

The project is now focussed on the final micro-optical interferometer design and the production of the probing wafer.

ACKNOWLEDGEMENTS

Several people have contributed to the present work. Uwe Zeitner from Fraunhofer IOF contributed to the interferometer design. Steffen Michael and Norbert Zeike have given input of great value to the mechanical design of the inspection system. Arne Røyset, Kari Anne Bakke, Jon Tschudi and Marion O'Farrell from SINTEF and Adam Stryk from WUT contributed to the theoretical and experimental investigations. The authors want to thank these people for their valuable contributions.

SMARTIEHS is a collaborative project funded under the Grant Agreement 223935 to the 7th Framework Program Objective 2007-3.6.

REFERENCES

- [1] Osten, W. (ed), [Optical inspection of Microsystems], Taylor and Francis, New York, (2006)
- [2] Gastinger, K., Løvhaugen, P., Skotheim, Ø., and Hunderi, O., "Multi-technique platform for dynamic and static MEMS-characterisation", Proc. SPIE 6616, 66163K (2007)
- [3] Petitgrand, S., Yahiaoui, R., Danaie, K., Bosseboeuf A., and Gilles, J.P. "3D measurement of micromechanical devices vibration mode shapes with a stroboscopic interferometric microscope", Optics and Lasers in Eng. 36, 77-101 (2001)
- [4] Gastinger, K., Kujawinska, M., Løvhaugen, O., Beer, S., Gorecki C., and Zeitner, U., "SMARTIEHS – Smart inspection system for high-speed and multifunctional testing of MEMS and MOEMS", Proc. 14th Micro Optics Conference 2008 (MOC'08) Brussels Vol. 14, 194-195 (2008)
- [5] Beer, S., Zeller, P., Blanc, N., Lustenberger, F., and Seitz, P., "Smart pixels for real-time optical coherence tomography", Proc. SPIE Vol. 5302, 21-32 (2004)
- [6] Michael, S., Kurth S. et al, "MEMS Parameter Identification on Wafer Level using Laser Doppler Vibrometer", Smart Systems Integration, Paris, 321-328 (2007)
- [7] Gorecki, C., Jóźwik, M., and Sałbut, L., "Multifunctional interferometric platform for on-chip testing the micromechanical properties of MEMS/MOEMS", J. Microlithography Microfabrication Microsystems 4(4), 1-10 (2005)
- [8] Kacperski, J., and Kujawinska, M., "Active LCoS based laser interferometer for microelements studies", Optics Express Vol. 14, 9664-9678 (2006)